Communication

Influence of Implant Base Material on Secondary Bone Healing: An In-Silico Study

Gargi Shankar Nayak *, Michael Roland, Björn Wiese, Norbert Hort, Stefan Diebels *

Posted Date: 26 September 2023

doi: 10.20944/preprints202309.1750.v1

Keywords: Bone remodelling; Mg implants; In-silico study; stress-shielding

Communication

Influence of Implant Base Material on Secondary Bone Healing: an *In-Silico* Study

Gargi Shankar Nayak [1,*], Michael Roland [1], Björn Wiese [2], Nobert Hort [2,3] and Stefan Diebels [1,*]

[1] Chair of Applied Mechanics, Saarland University, Campus A4 2, 66123 Saarbrücken, Germany
[2] Institute of Metallic Biomaterials, Helmholtz-Zentrum Hereon, Max-Planck-Str. 1, 21502 Geesthacht, Germany
[3] Leuphana University Lüneburg, Institute of Product and Process Innovation, Universitätsallee 1, D-21335 Lüneburg, Germany
* gargi.nayak@uni-saarland.de, s.diebels@mx.uni-saarland.de

Abstract: The type of implant at the fracture site has effects not only from biological perspective but also from mechanical perspective in fracture healing. Biodegradable implants such as magnesium (Mg) based alloys have shown faster secondary bone healing properties as compared to bioinert implants such as titanium (Ti). The general reasoning behind this is the benefit of Mg from biocompatibility perspectives. We study the effect of Ti and Mg as base materials for implants with their different mechanical properties. The focus of our work is on the displacements at the fracture site of the tibia and their influence on the stimulus for bone healing. We have found that in comparison to Ti, Mg implants have minimal *stress shielding* problem, only which led to better mechanical stimulus at the fracture site.

Keywords: bone remodelling; MG implants; *In-silico* study; stress-shielding

1. Introduction

The research work to repair bone-fracture has improved tremendously in the past years. Where, in the past only bioinert implants such as stainless steel (SLS) [1,2] and Ti [3,4] was applied for fracture healing, nowadays biodegradable implants such as Mg [5,6] and zinc (Zn) [7] are developing to replace/support them at a fast pace. Biodegradable implants have the advantage over bioinert implants in that they dissolve in the body over time during fracture healing [8]. Moreover, their low Young's modulus (E) also minimizes the *stress shielding* problem, generally seen with Ti and SLS implants, given their E value is significantly higher than that of bone [8].

In various references, the superior behaviour of Mg implants over inert metallic implants were observed on the basis of their better biological properties to enhance bone regeneration [9–11]. In the study performed by K. Jähn *et al.* the *in vivo* behaviour of Mg-2Ag and SS intramedullary nails on long bone fracture repair of mice was studied [10]. Mg-2Ag nails stimulated a faster bone formation as compared to SS nails, along with an augmented callus formation, which is necessary for a better secondary bone healing [12]. In another study, B. Acar *et al.* compared the clinical outcome of application of Mg and Ti screws for biplane chevron medical malleolar osteotomy on patients [13]. Interestingly, both the screws provided similar success. Moreover, as Mg screws degrade during the process, no implant removal operation is needed after the procedure, which is generally the case for Ti implants. However, the mechanical aspects of Mg implants for bone healing are not typically considered in these studies.

To understand the influence of mechanical conditions on fracture healing, L. E. Claes & C. A. Heigele have developed a tissue differentiation theory which portrayed the influence of local stress and strain conditions in the callus on its secondary healing regime [14]. The fracture healing in this approach takes two strains into account: octahedral shear strain that relates to the shape change in the callus and volumetric strain that relates to volume change in the callus. The interplay between these two strains determines the best conditions for bone formation. This theory has been used successfully in various simulation studies to predict the best conditions for fracture healing [15–17].

Preprints (www.preprints.org) | NOT PEER-REVIEWED | Posted: 26 September 2023 doi:10.20944/preprints202309.1750.v1

Thus, in this research work, this previous knowledge was used to develop a computational framework to visualize the difference in mechanical environment, based on the selection of implant base material. The implant placed at the Tibia fracture site was chosen as material Mg and Ti, and the mechanical conditions of the implant and fracture site were measured. This research work is a computational approach to understand the mechanical conditions, excluding the other (biological, chemical) ones to understand the influence of this aspect on fracture healing for the short term.

2. Materials and Methods

2.1. Implant Design

The implant strategy chosen for the simulation is shown in **Error! Reference source not found.**. The implant depicted comes from an in-house generated computer-aided design (CAD) dataset, based on a standard titanium locking compression plate (LCP) with ten holes and a length of 186 mm. The bone model is generated from a computed tomography (CT) scan of a human cadaveric specimen of a lower leg. The data set originates from the completed BMBF (German Federal Ministry of Education and Research) funded project "IIP-Extrem" (FKZ: 13GW0124). The donor was a female at the age of 74 with a body height of 152.4 cm (60 in.) and a body weight of 81.65 kg (180 lbs.) with no bone diseases. The CT scan was performed with a Siemens SOMATOM Definition Edge with a resolution of 0.541 mm as pixel spacing and 0.60 mm distance between two images. To guarantee a good representation of the local bone properties in the simulation models, a six-rod bone density calibration phantom (QRM-BDC/6, QRM GmbH Moehrendorf, Germany) was used during the CT scan.

The segmentation of the tibia and the calibration phantom in the image stack were performed in the image processing and model generation software ScanIP (Synopsys, Mountain View, CA, United States). The images were segmented into different masks (bone, single rods) with an adaptive threshold procedure, supplemented by a morphological close filter with isotropic values and a mask smoothing with a recursive Gaussian filter with anisotropic values resulting in a high segmentation quality without detectable problems.

Based on the calibration phantom, a linear regression was used to calibrate the grayscale values given in hounsfield units (HU) of the CT image stack and to compute the corresponding equivalent mineral density in each voxel of the bone mask. The calibrated equivalent mineral density values are then used to calculate the ash density values with the mapping given in [21] and the corresponding apparent density values with the equation from Edwards *et al.* [22]. In a subsequent step, the local bone properties were used to compute the local material parameters, i.e., E value and Poisson's ratio (ν) with the power law relationship from Rho *et al.* [18].

The fracture was generated via an image processing step in the ScanIP environment with a Boolean operation between different masks. As fracture, a simple oblique fracture in the diaphyseal segment at an angle of 30° to the tibial axis according to the international classification of the orthopaedic trauma association with AO/OTA 42A2 was chosen.

The material properties chosen for the implant are shown in **Error! Reference source not found.**. As the initial stages of bone healing was modelled, the callus properties were taken according to such conditions (soft tissue).

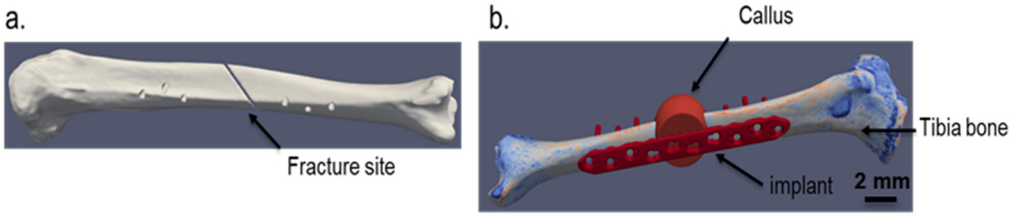

Figure 1. a. The fracture site, b. The implant design for the simulation.

Table 1. The material parameters taken for modelling of implant and callus [19].

Preprints (www.preprints.org) | NOT PEER-REVIEWED | Posted: 26 September 2023 doi:10.20944/preprints202309.1750.v1

Parameters	Ti	Mg	Callus
Young's modulus (GPa)	108	45	0.003
Poisson's ratio	0.36	0.28	0.40

2.2 Simulation Methodology

A linear elastic model was used for simulation. The simulation of the gait cycle was performed. The knee joint force data regarding to the gait cycle was taken from [20]. As in the initial stages after operation, the legs can sustain only up to 30% of the body weight [19], the force was adjusted according to these situations. The resulting gait data used for simulation can be seen in **Error! Reference source not found.**a. The simulation was performed in Abaqus/Explicit 2023 with the model from **Error! Reference source not found.**b.

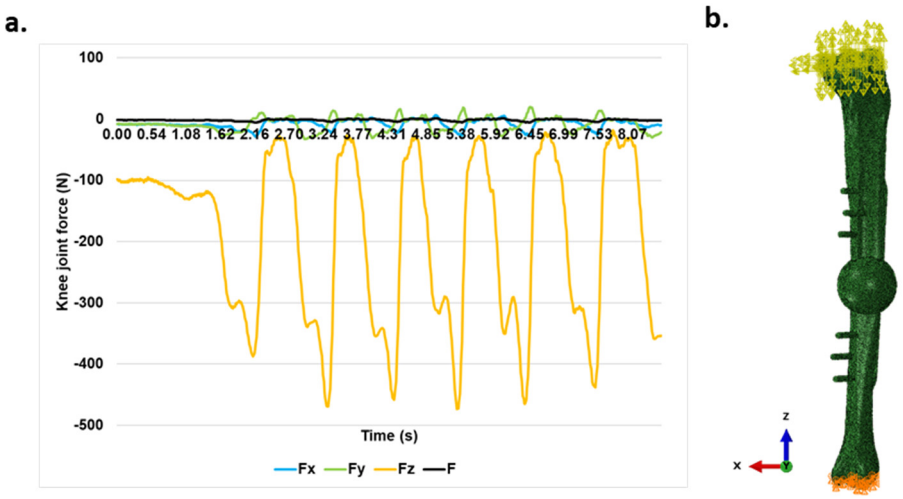

Figure 2. a. The gait cycle used in simulation; b. the direction of forces applied on the model, e.g. Fx corresponds to the force applied on the bone from x direction. .

The mechanobiological approach based on the tissue differentiation theory [14] was applied to determine the callus remodelling. The strain tensor was measured for each element in the callus and the octahedral shear strain and volumetric strain were calculated using a MATLAB code and evaluated according to the limits specified in the literatures [14,17] in Paraview. Moreover, the von Mises stress distribution in the implant was measured to compare the stress shielding tendency of these implants.

3. Results

The von Mises stress distribution in Mg and Ti implants has been shown in **Error! Reference source not found.** a& b. In Figure 3 c the overall stress distribution comparison during a gait cycle for both implants were illustrated. The corresponding engineering strain (**E**) distribution in implants and fracture sites can be seen in **Error! Reference source not found.**. The strain distribution on the top surface of the bone fragment from fracture site shown in **Error! Reference source not found.** was used for this visualization. It was found out that Mg played a lower role in load bearing, as compared to that of Ti. The load gets distributed at fracture site to a higher extent when Mg implants were used, which led to their higher strain values as compared to Ti.

Preprints (www.preprints.org) | NOT PEER-REVIEWED | Posted: 26 September 2023 doi:10.20944/preprints202309.1750.v1

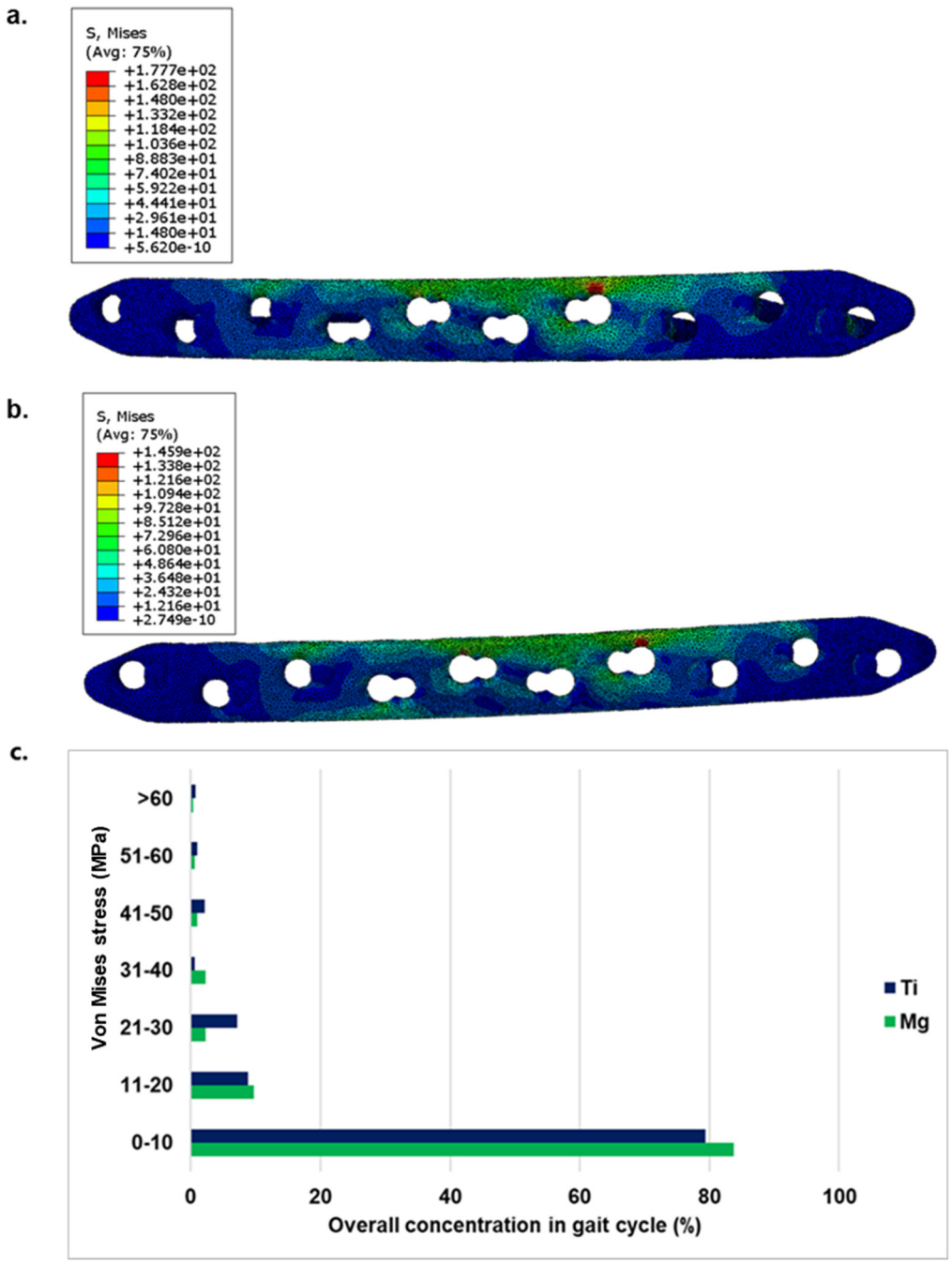

Figure 3. The von mises stress distribution in MPa for a. Ti and b. Mg implant at the same stage of a gait cycle; c. The overall stress distribution for Mg and Ti implants in a gait cycle. More stress was taken by Ti as compared to Mg. .

Preprints (www.preprints.org) | NOT PEER-REVIEWED | Posted: 26 September 2023 doi:10.20944/preprints202309.1750.v1

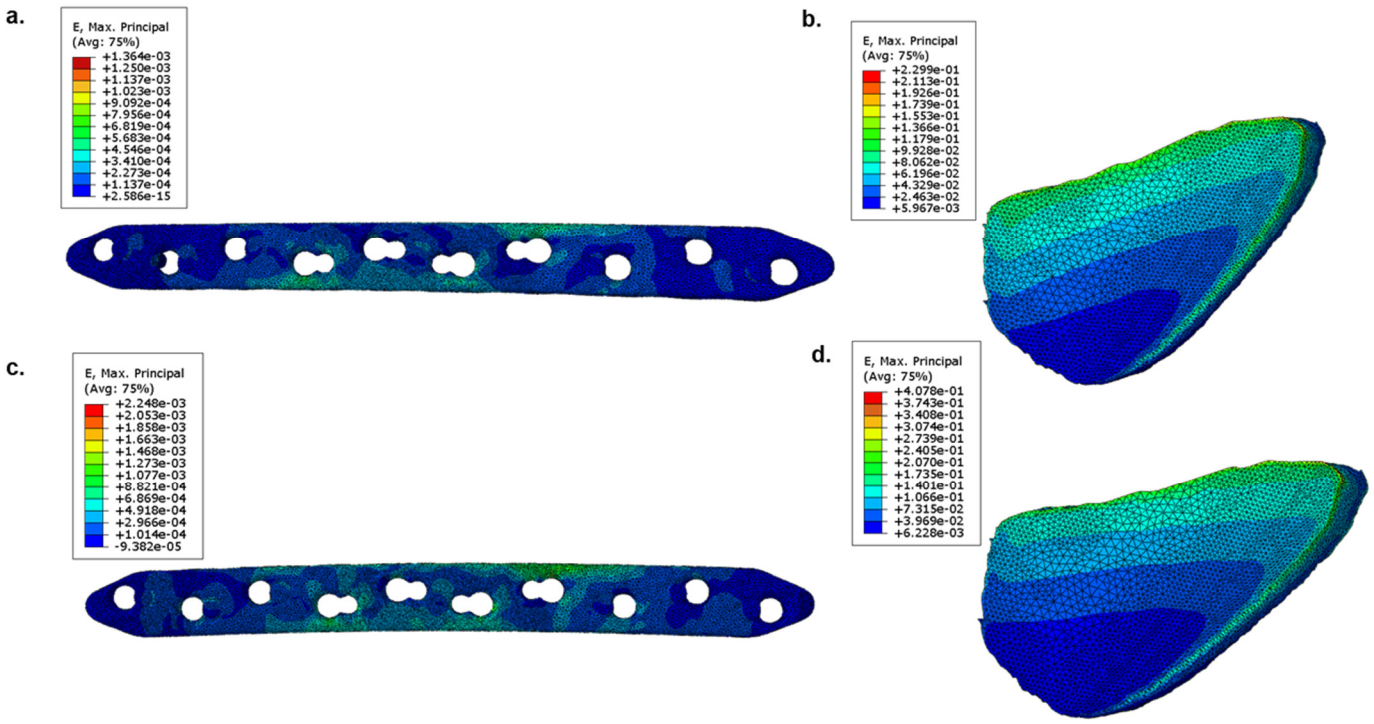

Figure 4. Engineering strain distribution in a. Ti implants and b. fracture site; c. Mg implants and d. fracture site in the same stage of a gait cycle. Higher strain values were found for both parts when Mg implants were used.

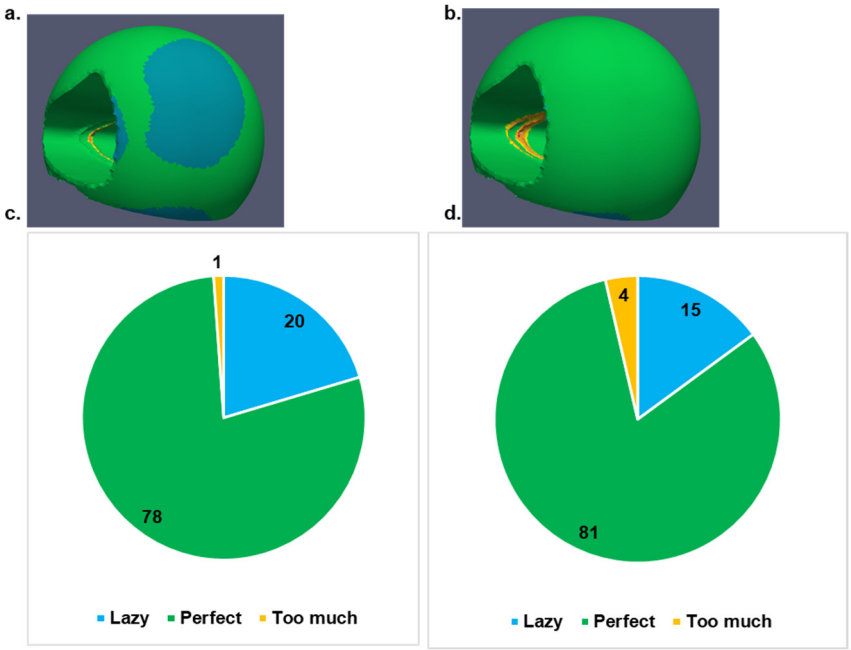

Figure 5. The mechanical stimulus distribution in the callus at the same stage of a gait cycle for a. Ti and b. Mg implant; the overall mechanical stimulus distribution percentage in callus for c. Ti, and d. Mg implant in a gait cycle. The better mechanical stimulus for bone development was found when Mg was used as implant.

The secondary healing conditions via mechanical stimulus were visualized for the callus, considering both implants as can be seen in **Error! Reference source not found.**. Based on the strain stimulus, lazy corresponds to the condition where too low stimulus could lead to removal of callus causing delayed or failed bone healing, perfect stimulus

 doi:10.20944/preprints202309.1750.v1

corresponds to the best conditions to achieve maximal healing potential of the tissues, and too much stimulus corresponds to possible danger in fracture healing due to macroscopic movements of the neighbouring bones that can cause refracture of the hard callus. The callus showed higher possibility for secondary healing when Mg implants was used.

On the implant side, the minimum as well as the maximum stress in the Mg implant (max. 117 MPa) is lower than in the Ti implant (max. 163 MPa). The stress is distributed over a larger area in the Mg implant and thus the force is absorbed more evenly over the implant than in the Ti case.

4. Discussion

To evaluate the suitability of Mg implants in hard tissue replacement applications, this *in silico* study has been performed. The conditions at the initial phase after implantation has been simulated. Ti took the majority of load which was not the case for Mg. In the simulation of the gait cycle, where Mg led to higher stress concentration in the range of 0-20 MPa than that of Ti, Ti had upper hand for the higher concentration range. Moreover, the maximum von Mises stress in Ti implant was found out to be 163 MPa as compared to 117 MPa in Mg implant. The *stress shielding* problem is highly associated with rigidity metallic implants such as Ti, given to their high *E* value (108 GPa) for a given geometry. This was also seen in the simulation results. Due to high *E* value, Ti has considerably lower strain than that of Mg for the same amount of stress, thus for majority of the loading conditions, bone doesn't experience any load. This led to minimal strain at fracture site for Ti implants. The *E* of Mg (45 GPa) is significantly closer to bone (~ 20 GPa) [21], thus it can act as a proper support for the bone where a better mechanical stimulus for bone healing can be achieved. This was also verified for non-degradable Ti-based implants [22,23]. Nails made of two Ti alloys were investigated, one with a high-rigidity (Ti-6Al-4V with 110 GPa) and one with a low-rigidity (Ti-24Nb-4Zr-7.9Sn with 33 GPa). In this study, the influence of the lower rigidity on better external callus formation and a reduced bone resorption than the high-rigidity nail was determined. Mg alloys have a similarly lower *E* and would contribute an additional beneficial biological effect on healing [24,25].

To evaluate the secondary healing conditions of the callus, the aforementioned tissue differentiation theory was applied. The strain stimulus was based on the distribution of octahedral shear strain and hydrostatic strain in the callus. The results supported the previous study, where Mg nails augmented the callus formation in *in vivo* studies [10]. The influence of the mechanical properties of the implant on the callus growth was clearly seen in the results. As Ti absorbed part of the major mechanical stress, the callus did not have the higher chance of secondary healing which was not the case for Mg implants. Similar results were also found by N. Fouda *et al.* in the simulation study where SS and Carbon/hydroxyapatite (C/HA) were compared for better fracture healing of tibia [26]. In that study, lower stress shielding of C/HA was given to be the major factor behind better secondary healing than SS implant. The Mg implants also have advantage in terms of its biodegradability that along with favouring the superior bone healing conditions also limit the need for implant removal operation.

Nonetheless, the results in this study only corresponds to the initial phase after implantation. The influence of Mg degradation in long term study has not been performed in this study. The correlation between Mg degradation and new bone formation throughout the bone remodeling phase is needed to be simulated to understand the best possible condition needed for the implant to degrade with minimal negative influence on bone reformation.

5. Conclusions

In this study, the initial phase of bone healing at tibia fracture site was simulated. The influence of the implant material on stimulus required for development of callus into bone was investigated,

where Mg was compared with Ti. The loading conditions in tibia during gait cycle were used as input. The lower stiffness of Mg implant helped in providing better mechanical stimulus for bone formation in callus. As Ti implant took major amount of load, the callus was seen to have little lower stimulus which can delay healing. This was also confirmed by the von Mises stress distribution in these two implants during the gait cycle.

However, as Mg is a biodegradable implant, this study only confirms the initial phase of bone healing. In the next phase of this study, the biodegradability of the Mg will be coupled in this model to provide a better overview about the possibility of applying Mg implant to repair tibia fracture in a long term.

Author Contributions: Conceptualization, S. Diebels and B. Wiese.; methodology, M. Roland; validation, G. S. Nayak.; writing—original draft preparation, G. S. Nayak.; writing—review and editing, G. S. Nayak, B. Wiese, M. Roland, S. Diebels, N. Hort; visualization, G. S. Nayak, M. Roland.; supervision, S. Diebels and N. Hort. All authors have read and agreed to the published version of the manuscript.

Funding: This research received no external funding.

Data Availability Statement: The data presented in this study could be obtained on request from the corresponding author.

Conflicts of Interest: The authors declare no conflict of interest.

References

1. S. De Fátima Ferreira Mariotto, V. Guido, L.Y. Cho, C.P. Soares, K.R. Cardoso, Porous stainless steel for biomedical applications, Materials Research. 14 (2011) 146–154. https://doi.org/10.1590/S1516-14392011005000021.
2. A. Goharian, M.R. Abdullah, Bioinert Metals (Stainless Steel, Titanium, Cobalt Chromium), Elsevier Inc., 2017. https://doi.org/10.1016/b978-0-12-804634-0.00007-0.
3. M. McCracken, Dental implant materials: Commercially pure titanium and titanium alloys, Journal of Prosthodontics. 8 (1999) 40–43. https://doi.org/10.1111/j.1532-849X.1999.tb00006.x.
4. H.J. Rack, J.I. Qazi, Titanium alloys for biomedical applications, Materials Science and Engineering C. 26 (2006) 1269–1277. https://doi.org/10.1016/j.msec.2005.08.032.
5. M. Razavi, M.H. Fathi, M. Meratian, Fabrication and characterization of magnesium-fluorapatite nanocomposite for biomedical applications, Mater Charact. 61 (2010) 1363–1370. https://doi.org/10.1016/j.matchar.2010.09.008.
6. Y. Zheng, Magnesium Alloys as Degradable Biomaterials, 2015. https://doi.org/10.1201/b18932.
7. E. Farabi, J. Sharp, A. Vahid, J. Wang, D.M. Fabijanic, M.R. Barnett, S. Corujeira Gallo, Novel Biodegradable Zn Alloy with Exceptional Mechanical and in Vitro Corrosion Properties for Biomedical Applications, ACS Biomater Sci Eng. 7 (2021) 5555–5572. https://doi.org/10.1021/acsbiomaterials.1c00763.
8. M.I.Z. Ridzwan, S. Shuib, Hassan A. Y., A.A. Shokri, M.N. Mohamad Ibrahim, Problem of Stress Shielding and Improvement to the Hip Implant Designs: A review, J Med Sci. 7 (2007) 460–467.
9. N. Li, Y. Zheng, Novel Magnesium Alloys Developed for Biomedical Application: A Review, J Mater Sci Technol. 29 (2013) 489–502. https://doi.org/10.1016/j.jmst.2013.02.005.
10. K. Jähn, H. Saito, H. Taipaleenmäki, A. Gasser, N. Hort, F. Feyerabend, H. Schlüter, J.M. Rueger, W. Lehmann, R. Willumeit-Römer, E. Hesse, Intramedullary Mg2Ag nails augment callus formation during fracture healing in mice, Acta Biomater. 36 (2016) 350–360. https://doi.org/10.1016/j.actbio.2016.03.041.
11. H.Y. López, D.A. Cortés-Hernández, S. Escobedo, D. Mantovani, In Vitro Bioactivity Assessment of Metallic Magnesium, Key Eng Mater. 309–311 (2006) 453–456. https://doi.org/10.4028/www.scientific.net/kem.309-311.453.
12. A. Bigham-Sadegh, A. Oryan, Basic concepts regarding fracture healing and the current options and future directions in managing bone fractures, Int Wound J. 12 (2015) 238–247. https://doi.org/10.1111/iwj.12231.
13. B. Acar, O. Kose, M. Unal, A. Turan, Y.A. Kati, F. Guler, Comparison of magnesium versus titanium screw fixation for biplane chevron medial malleolar osteotomy in the treatment of osteochondral lesions of the talus, European Journal of Orthopaedic Surgery and Traumatology. 30 (2020) 163–173. https://doi.org/10.1007/s00590-019-02524-1.
14. L.E. Claes, C.A. Heigele, Magnitudes of local stress and strain along bony surfaces predict the course and type of fracture healing, 1999.
15. B.J. Braun, M. Orth, S. Diebels, K. Wickert, A. Andres, J. Gawlitza, A. Bücker, T. Pohlemann, M. Roland, Individualized Determination of the Mechanical Fracture Environment After Tibial Exchange Nailing—A Simulation-Based Feasibility Study, Front Surg. 8 (2021). https://doi.org/10.3389/fsurg.2021.749209.
16. M. Orth, B. Ganse, A. Andres, K. Wickert, E. Warmerdam, M. Müller, S. Diebels, M. Roland, T. Pohlemann, Simulation-based prediction of bone healing and treatment recommendations for lower leg fractures:

Effects of motion, weight-bearing and fibular mechanics, Front Bioeng Biotechnol. 11 (2023). https://doi.org/10.3389/fbioe.2023.1067845.
17. S.J. Shefelbine, P. Augat, L. Claes, U. Simon, Trabecular bone fracture healing simulation with finite element analysis and fuzzy logic, J Biomech. 38 (2005) 2440–2450. https://doi.org/10.1016/j.jbiomech.2004.10.019.
18. J. Rho, M. Hobatho, Relations of mechanical properties to density and CT numbers in human bone, Med. Eng. Whys. 17 (1995) 347–355.
19. A. Sorriento, M. Chiurazzi, L. Fabbri, M. Scaglione, P. Dario, G. Ciuti, A novel capacitive measurement device for longitudinal monitoring of bone fracture healing, Sensors. 21 (2021). https://doi.org/10.3390/s21196694.
20. G. Bergmann, A. Bender, F. Graichen, J. Dymke, A. Rohlmann, A. Trepczynski, M.O. Heller, I. Kutzner, Standardized loads acting in knee implants, PLoS One. 9 (2014). https://doi.org/10.1371/journal.pone.0086035.
21. M. Cuppone, B.B. Seedhom, E. Berry, A.E. Ostell, The Longitudinal Young's Modulus of Cortical Bone in the Midshaft of Human Femur and its Correlation with CT Scanning Data, in: Calcif Tissue Int, 2004: pp. 302–309. https://doi.org/10.1007/s00223-002-2123-1.
22. M. Sha, Z. Guo, J. Fu, J. Li, C.F. Yuan, L. Shi, S.J. Li, The effects of nail rigidity on fracture healing in rats with osteoporosis, Acta Orthop. 80 (2009) 135–138. https://doi.org/10.1080/17453670902807490.
23. A. Bigham-Sadegh, A. Oryan, Basic concepts regarding fracture healing and the current options and future directions in managing bone fractures, Int Wound J. 12 (2015) 238–247. https://doi.org/10.1111/iwj.12231.
24. H. Zhou, B. Liang, H. Jiang, Z. Deng, K. Yu, Magnesium-based biomaterials as emerging agents for bone repair and regeneration: from mechanism to application, Journal of Magnesium and Alloys. 9 (2021) 779–804. https://doi.org/10.1016/j.jma.2021.03.004.
25. A. Burmester, R. Willumeit-Römer, F. Feyerabend, Behavior of bone cells in contact with magnesium implant material, J Biomed Mater Res B Appl Biomater. 105 (2017) 165–179. https://doi.org/10.1002/jbm.b.33542.
26. N. Fouda, R. Mostafa, A. Saker, Numerical study of stress shielding reduction at fractured bone using metallic and composite bone-plate models, Ain Shams Engineering Journal. 10 (2019) 481–488. https://doi.org/10.1016/j.asej.2018.12.005.